Oncology and Cancer Research using ImageStream Cytometry

The ImageStream system combines high-speed image capture with image quantification to create a statistically powerful microscopy platform, enabling robust discrimination of cells based on their appearance. This document highlights applications of ImageStream cytometry to the field of oncology as described in publications, posters and podium presentations. For more information, check out the website: (https://www.amnis.com/oncology.html)

Table of Contents:

Etoposide-induced cell death in prostate cancer cell lines

Summary: This ImageStream assay quantifies apoptosis using the morphology of the nuclear image. Cells with condensed (reduced nuclear area) and fragmented (increased nuclear texture, Spot Small Total) nuclei are discriminated by gating (a), with representative apoptotic cells shown at right. Note that some cells with fragmented nuclei were AnnexinV negative (c).

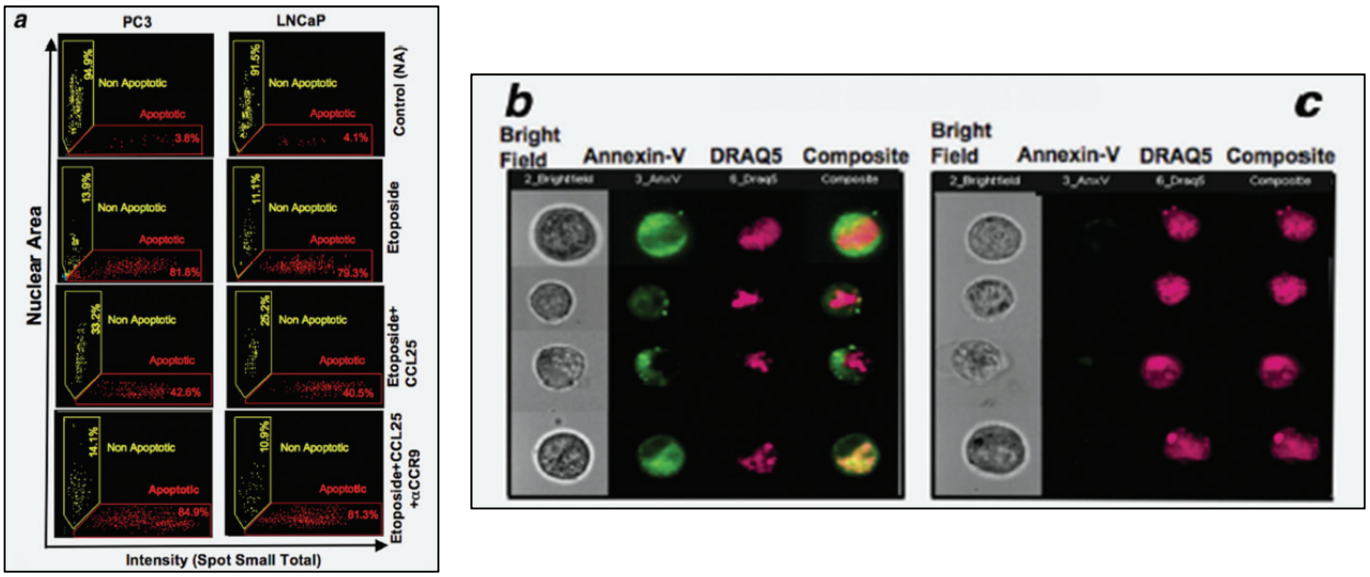

"PCa cells treated with etoposide showed 81.8% (PC3) and 79.3% (LNCaP) apoptosis, in comparison to the untreated cells, which showed only 3.8% and 4.1% apoptotic cells, respectively (Fig. 1a). Interestingly, apoptosis induced by etoposide alone in PC3 and LNCaP cells was significantly ($p < 0.001$) inhibited in presence of CCL25 (42.6% and 40.5%, respectively). Furthermore, inhibition of etoposide-induced apoptosis in presence of CCL25 was blocked when CCL25 and CCR9 interaction was inhibited using anti-CCR9 antibody (Fig. 1a). These findings suggest that the CCR9-CCL25 axis promotes PCa cell survival by inhibiting apoptosis."

Reference: Praveen, K.S., S. Rajesh, R.N. Kristian, W.E. John, E.G. William, and S. Shailesh, *CCR9 mediates PI3K/AKT-dependent antiapoptotic signals in prostate cancer cells and inhibition of CCR9-CCL25 interaction enhances the cytotoxic effects of etoposide.* International Journal of Cancer, 2010. **127**(9): p. 2020–2030.

~ ~ ~ ~ ~ ~

EGFR clustering in breast cancer cells

Summary: This ImageStream assay measures receptor clustering using the morphology of the Epidermal Growth Factor Receptor (EGFR) image. Cells with clustered EGFR (pink gate at left, images at far right) have lower EGFR area and higher texture (Bright Detail Intensity) values compared to cells with uniform membrane distributions (green gate at left).

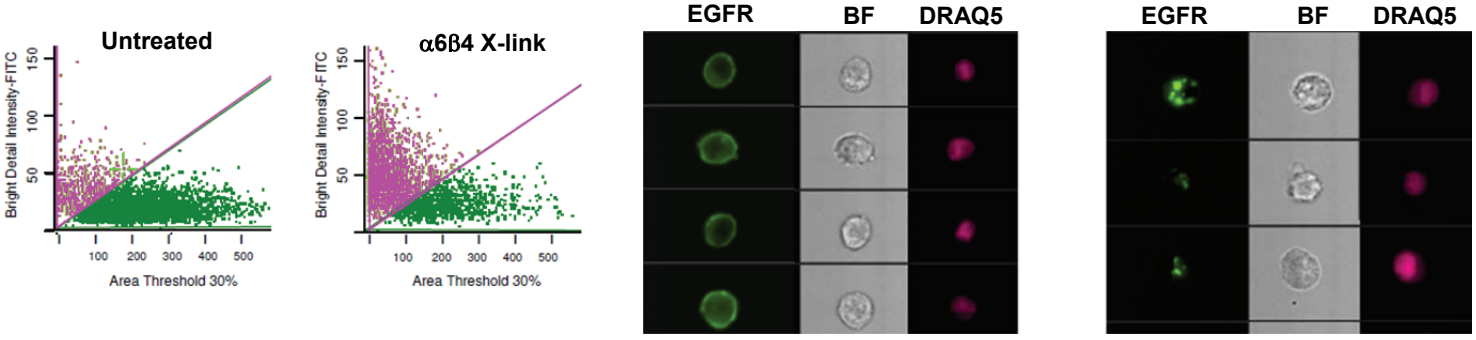

"Crosslinking α6β4 integrin in breast carcinoma cells induces (EGFR) clustering and preferentially promotes Rho activation in response to EGF. We hypothesize that this integrin-EGFR crosstalk may facilitate tumor cell cytoskeletal rearrangements important for tumor progression."

Reference: Gilcrease, M.Z., X. Zhou, X. Lu, W.A. Woodward, B.E. Hall, and P.J. Morrissey, *Alpha6beta4 integrin crosslinking induces EGFR clustering and promotes EGF-mediated Rho activation in breast cancer.* J Exp Clin Cancer Res, 2009. **28**: p. 67.

uPAR-induced phagocytosis of apoptotic tumor cell fragments

Summary: This ImageStream assay measures the binding and internalization of apoptotic T cell tumor fragments (PKH26) by CS-1 phagocytic cells (GFP+) transfected with Urokinase Plasminogen Activator Receptor (uPAR), β5 integrin, or mock (pCx). Internalization is uniquely measured by quantifying the intensity of the apoptotic material specifically within the internal compartment of the CS-1 cells.

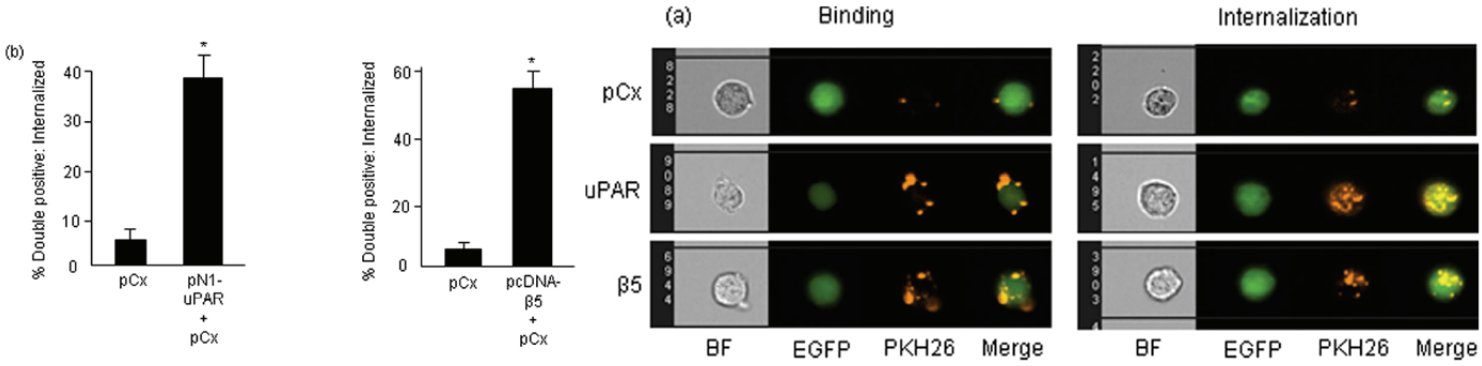

"In the present study, we report that uPAR has a dominant role in the efferocytosis of apoptotic cells, promoting engulfment of apoptotic corpses in transiently overexpressing model phagocytes as well as in breast cancer lines that acquire increased expression of uPAR by epigenetic changes. Because uPAR and the plasminogen activator system are often overexpressed in malignant epithelial carcinomas that include breast, prostate, colon, brain, and others, these data imply that uPAR might confer a phagocytic advantage of uPAR-expressing tumor cells in the tumor microenvironment."

Reference: D'Mello, V., S. Singh, Y. Wu, and R.B. Birge, *The urokinase plasminogen activator receptor promotes efferocytosis of apoptotic cells.* J Biol Chem, 2009. **284**(25): p. 17030-8.

~ ~ ~ ~ ~ ~

Nanoparticle loading in target cell populations

Summary: This ImageStream assay measures heterogeneity in the amount of nanonparticles loaded during dosing of U2-OS cells. This paper also uses the ImageStream to show that partitioning of nanoparticles in cell division is random and asymmetric. These phenomena have implications for the use of nanoparticle therapeutic drug delivery strategies in oncology.

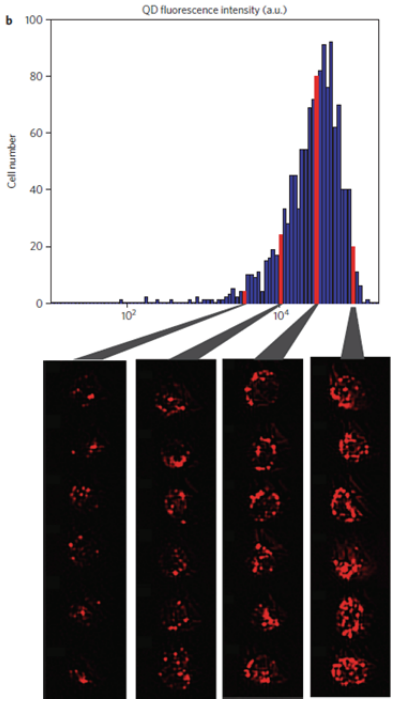

"Examples of cell images corresponding to specific bins within an intensity histogram of 5,000 cells are shown in Fig. 2b. The wide distribution of fluorescence intensity suggests that there are varying numbers of nanoparticle-loaded vesicles (NLVs) across the cell population; loading of cells with a single concentration can result in a wide variation in the number of nanoparticle clusters that attach to the cell membrane, even when peptides are used to target cells. In the context of nanotoxicology, this implies that arange of cellular response is possible from a single dose of toxin."

Reference: Summers, H.D., P. Rees, M.D. Holton, M. Rowan Brown, S.C. Chappell, P.J. Smith, and R.J. Errington, *Statistical analysis of nanoparticle dosing in a dynamic cellular system.* Nat Nanotechnol, 2011. **6**(3): p. 170-4.

Ofatumamab-mediated complement fixation

Summary: This ImageStream assay measures co-localization of C1q to therapeutic antibody on the surface of B cell tumor cells, indicating that Ofatumamab (OFA) mediates complement fixation. This conclusion is made possible because the ImageStream a) rapidly collects thousands of images per sample for good statistics and b) objective quantifies co-localization on a per-cell basis using the bright detail similarity score.

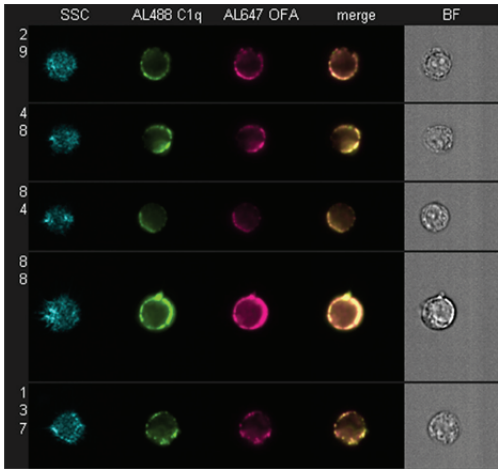

Table I. *Binding of Al488-labeled C1q to mAb-opsonized Daudi cells and colocalization of C1q with mAb*

	Expt. 1			Expt. 2			Expt. 3[a]		
	Al647 mAb (GMF)	Al488 C1q (GMF)	BDSS	Al647 mAb (GMF)	Al488 C1q (GMF)	BDSS	Al647 mAb (GMF)	Al488 C1q (GMF)	BDSS
Al647 OFA	181,000	162,000	3.0	116,000	113,000	3.4	206,000	30,000	2.5
Al647 RTX	186,000	7,500	0.9	61,000	6,600	2.1	155,000	2,200	1.0
Al647 7D8[b]	133,000	2,300	0.6	104,000	1,000	0.9	210,000	1,300	0.7

[a] Different Al488 C1q preparation.
[b] IgG4 (K322A).
BDSS, Bright detail similarity score; GMF, geometric mean fluorescence.

"To test for colocalization quantitatively, double-positive cells (Fig. 2C) were analyzed for colocalization based on an algorithm that calculates the bright detail similarity score. Values of 3–3.5 indicate substantial colocalization, and values of 2.5–3 indicate moderate colocalization. The results of three independent experiments (Table I) reveal that Al488 C1q bound to Al647 OFA-opsonized cells is indeed colocalized with bound OFA."

Reference: Pawluczkowycz, A.W., F.J. Beurskens, P.V. Beum, M.A. Lindorfer, J.G. van de Winkel, P.W. Parren, and R.P. Taylor, *Binding of submaximal C1q promotes complement-dependent cytotoxicity (CDC) of B cells opsonized with anti-CD20 mAbs ofatumumab (OFA) or rituximab (RTX): considerably higher levels of CDC are induced by OFA than by RTX.* J Immunol, 2009. **183**(1): p. 749-58.

~ ~ ~ ~ ~ ~

Rituxan-mediated monocyte trogocytosis of B cell tumor membrane components

Summary: This ImageStream assay measures the therapeutic antibody-induced transfer of membrane components from Raji B cell tumor cells to monocytes. Using the CD14 image, the THP-1 and Raji-associated PKH26 and CD20 can be discriminated from each other within each conjugate, allowing measurement of rituxan-induced shaving reaction.

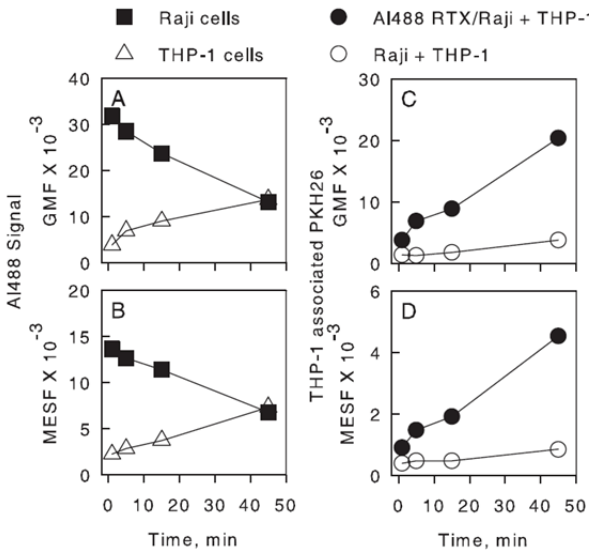

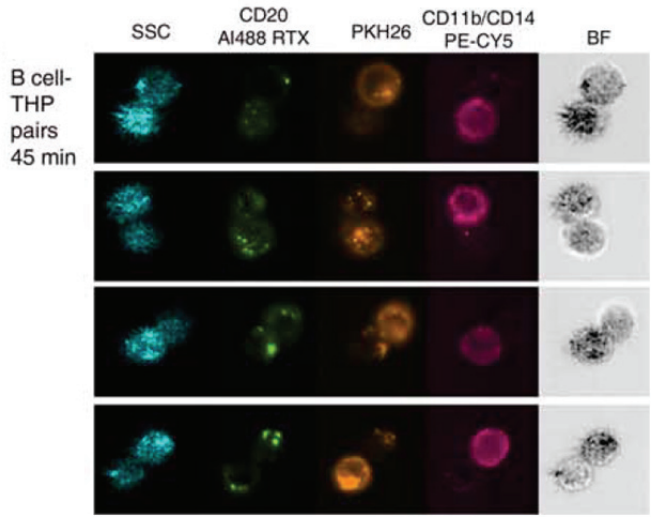

"Loss of Al488 signal by Raji cells (filled squares) is correlated with gain of Al488 signal by THP-1 cells (open triangles). Uptake of PKH26 signal by THP-1 cells from Al488 RTX-opsonized Raji cells is shown by the filled circles; uptake from nonopsonized Raji cells is shown by the open circles."

Reference: Beum, P.V., D.A. Mack, A.W. Pawluczkowycz, M.A. Lindorfer, and R.P. Taylor, *Binding of rituximab, trastuzumab, cetuximab, or mAb T101 to cancer cells promotes trogocytosis mediated by THP-1 cells and monocytes.* J Immunol, 2008. **181**(11): p. 8120-32.

~ ~ ~ ~ ~ ~

RA-induced nuclear translocation of Raf in myelomonocytic leukemia cells

Summary: This ImageStream assay measures Raf1 nuclear localization (by quantifying the similarity between the Raf and nuclear images on a per-cell basis) in HL60 cells differentiating in retinoic acid (RA) or tissue plasminogen activator (TPA) spiked media.

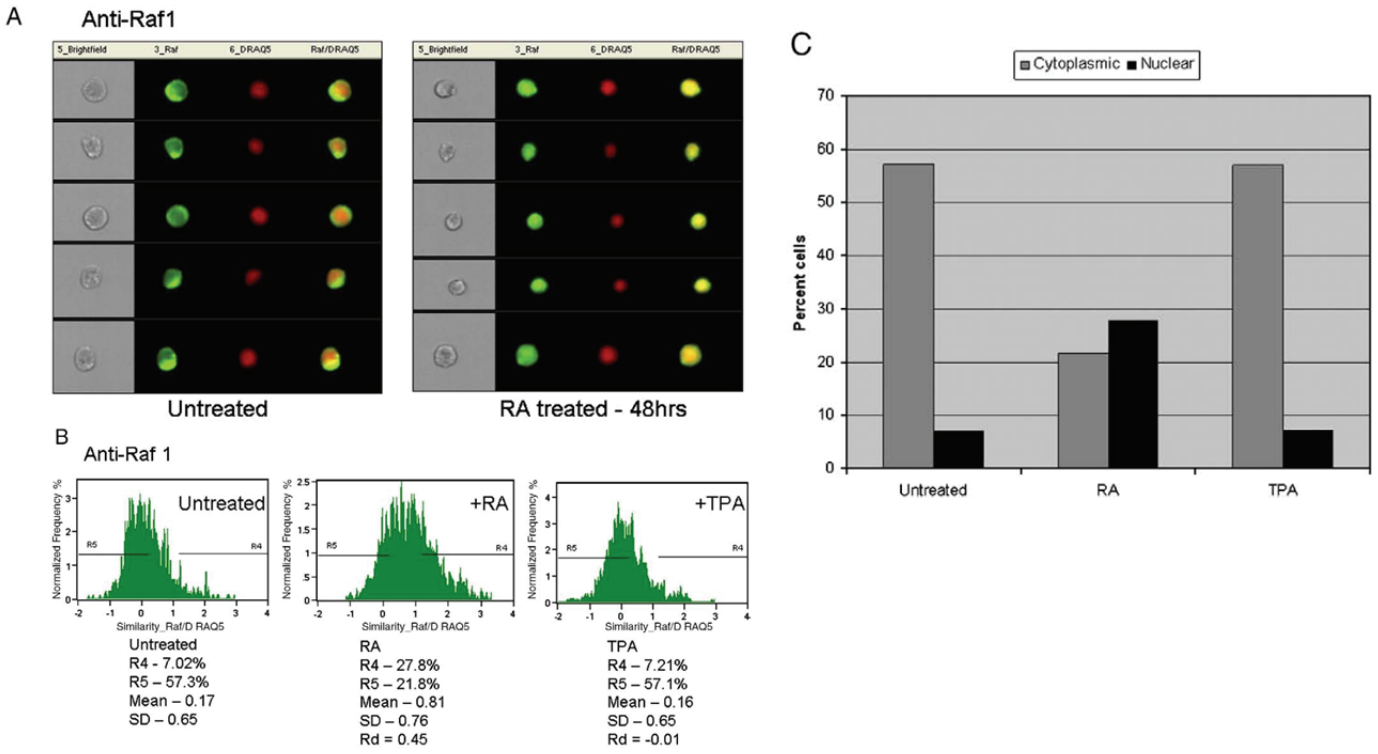

"Differentiating cells in RA induces a quantifiable increase in Raf1 nuclear localization (Rd 0.45). By contrast TPA, which is a known activator of Raf, fails to cause nuclear localization (Rd −0.01), suggesting a novel regulatory mechanism for Raf1 during RA-induced differentiation."

Reference: Smith, J., R.P. Bunaciu, G. Reiterer, D. Coder, T. George, M. Asaly, and A. Yen, *Retinoic acid induces nuclear accumulation of Raf1 during differentiation of HL-60 cells.* Exp Cell Res, 2009.

Correlating class I and adhesion molecule expression to KHSV load

Summary: This ImageStream assay simultaneously measures Karposi's sarcoma-associated herpesvirus (KHSV) load (by quantifiying the number of nuclear LANA spots per cell) and expression of cell surface makers in BCBL-1 cells, demonstrating that increased viral load is correlated with downregulation of MHC-I and ICAM-1 cell.

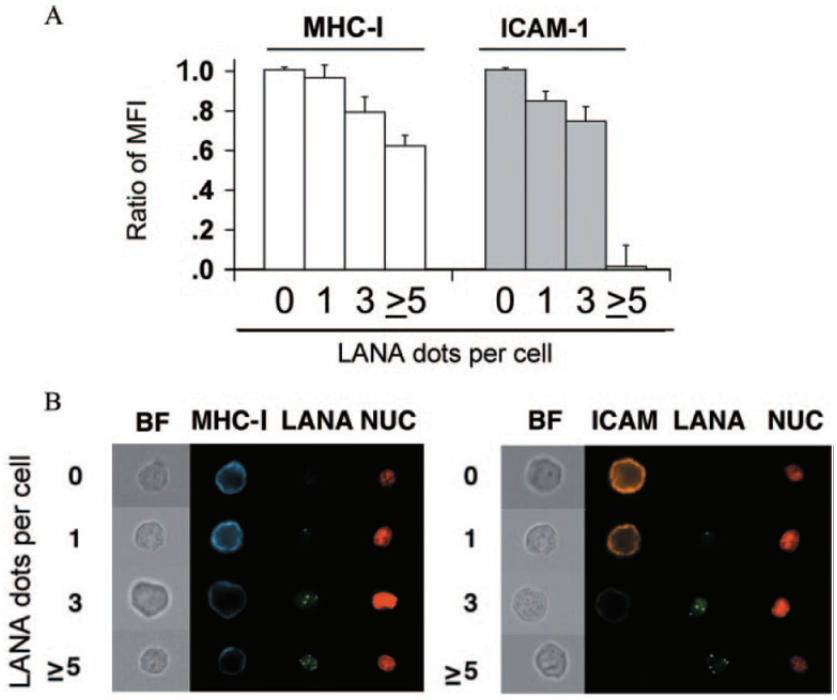

"In this study, we investigated the role of intracellular viral load and low-level MIR2 expression in KHSV-induced immune regulatory protein downregulation. Previous reports have explored the role of MIR2 through transfection studies or following lytic induction (10, 16, 17, 24, 30). The present data demonstrate that low-level de novo infection leads to expression of MIR2 levels sufficient for the detectable downregulation of immunological synapse components, MHC-I and ICAM-1."

Reference: Adang, L.A., C. Tomescu, W.K. Law, and D.H. Kedes, *Intracellular Kaposi's sarcoma-associated herpesvirus load determines early loss of immune synapse components.* J Virol, 2007. **81**(10): p. 5079-90.

Morphology-based identification of APML

Summary: This ImageStream assay uses the modulation texture feature to objectively discriminate the bright punctate pattern of promyelocytic leukemia protein (PML) associated with normal cells (C and E) from the diffuse pattern associated with APML (D and F). Automated collection of several thousand cells per patient sample enables reporting the percent of cells with aggregated PML as an indicator for APML risk.

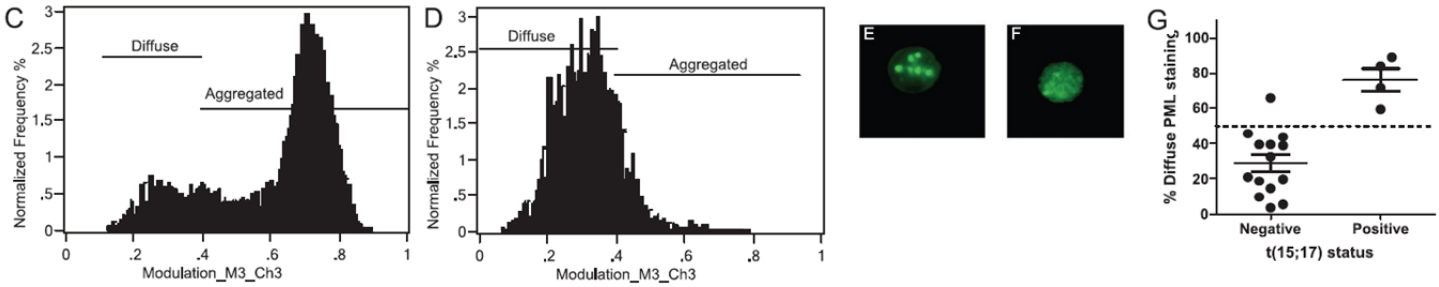

"Acute promyelocytic leukaemia (APML) can be promptly diagnosed by detecting abnormal diffuse staining patterns of PML bodies in abnormal promyelocytes using immunofluorescence microscopy. However, this technique is subjective, with low sensitivity. Using samples from 18 patients with acute myeloid leukaemia (AML) (including four with APML), the authors investigated whether imaging flow cytometry could be a viable alternative to this current technique and improve sensitivity levels. Bone marrow/peripheral blood cells were stained with an antibody to PML, and data were acquired on an ImageStream (Amnis Corporation, Seattle, Washington, USA). Using the modulation feature for data analysis, the authors demonstrated that this technique could successfully identify cases of APML. Imaging flow cytometry, by analysing greater numbers of cells and with the potential to include disease-specific antigens, increases the sensitivity of the current immunofluorescence technique. Imaging flow cytometry is an exciting technology that has many possible applications in the diagnosis of haematological malignancies, including the potential to integrate modalities."

Reference: Grimwade, L., E. Gudgin, D. Bloxham, M.A. Scott, and W.N. Erber, *PML protein analysis using imaging flow cytometry.* J Clin Pathol, 2010.

~ ~ ~ ~ ~ ~ ~

CTC detection

Summary: This ImageStream assay combines conventional circulating tumor cell (CTC) immunophenotyping strategies with high resolution imagery for definitive identification of rare tumor cells in whole blood samples. The multiple imaging channels provided by the system afford the opportunity for further functional and phenotypic characterization of CTC.

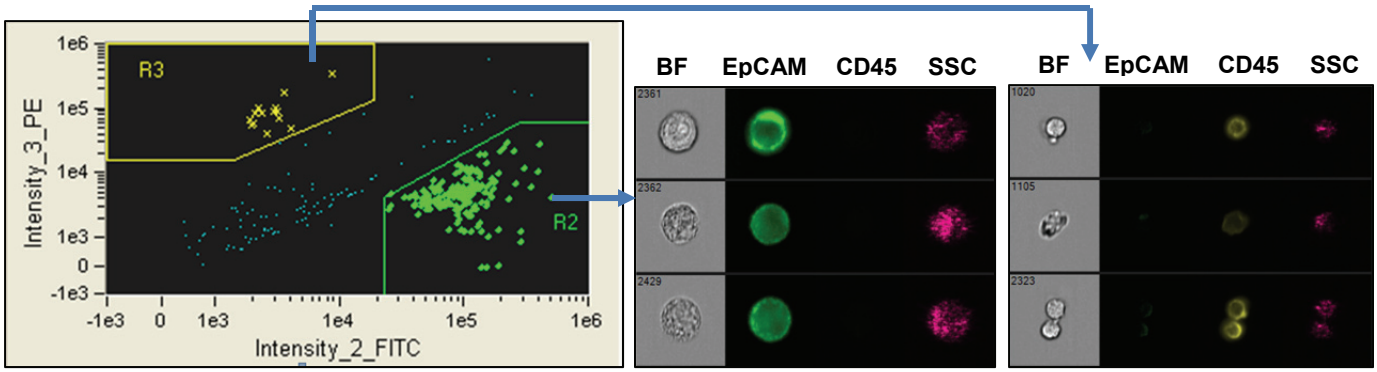

1 mL whole blood spiked with 500 CAMA epithelial tumor cells were enriched using RosetteSep™ CTC Enrichment Cocktail (Stem Cell Tech) and stained with FITC-conjugated anti-epithelial cell antibody (5E11, Stem Cell Tech) and PE-conjugated anti-CD45. The stained samples were then analyzed using an ImageStreamX.

Reference: Presentation at Circulating Tumor Cell Isolation and Diagnostics, 2011, Leiden, NL *Circulating Tumor Cell Detection and Characterization Using the Amnis ImageStreamX System* D Basiji, W Ortyn, CZimmerman, V Venkatachalam, T George, R Kong: http://www.amnis.com/documents/posters/11-001-1-pos%20Lorentz%20CTC.pdf

Reference list – Oncology applications for the ImageStream

Altman, B.J., S.R. Jacobs, E.F. Mason, R.D. Michalek, A.N. Macintyre, J.L. Coloff, O. Ilkayeva, W. Jia*, et al.*, *Autophagy is essential to suppress cell stress and to allow BCR-Abl-mediated leukemogenesis.* Oncogene, 2010.

Beum, P.V., D.A. Mack, A.W. Pawluczkowycz, M.A. Lindorfer, and R.P. Taylor, *Binding of rituximab, trastuzumab, cetuximab, or mAb T101 to cancer cells promotes trogocytosis mediated by THP-1 cells and monocytes.* J Immunol, 2008. **181**(11): 8120-32.

Degtyarev, M., A. De Maziere, C. Orr, J. Lin, B.B. Lee, J.Y. Tien, W.W. Prior, S. van Dijk*, et al.*, *Akt inhibition promotes autophagy and sensitizes PTEN-null tumors to lysosomotropic agents.* J Cell Biol, 2008. **183**(1): 101-16.

D'Mello, V., S. Singh, Y. Wu, and R.B. Birge, *The urokinase plasminogen activator receptor promotes efferocytosis of apoptotic cells.* J Biol Chem, 2009. **284**(25): 17030-8.

Gandillet, A., S. Park, F. Lassailly, E. Griessinger, J. Vargaftig, A. Filby, T.A. Lister, and D. Bonnet, *Heterogeneous sensitivity of human acute myeloid leukemia to beta-catenin down-modulation.* Leukemia, 2011.

Gilcrease, M.Z., X. Zhou, X. Lu, W.A. Woodward, B.E. Hall, and P.J. Morrissey, *Alpha6beta4 integrin crosslinking induces EGFR clustering and promotes EGF-mediated Rho activation in breast cancer.* J Exp Clin Cancer Res, 2009. **28**: 67.

Grimwade, L., E. Gudgin, D. Bloxham, M.A. Scott, and W.N. Erber, *PML protein analysis using imaging flow cytometry.* J Clin Pathol, 2010.

Henery, S., T. George, B. Hall, D. Basiji, W. Ortyn, and P. Morrissey, *Quantitative image based apoptotic index measurement using multispectral imaging flow cytometry: a comparison with standard photometric methods.* Apoptosis, 2008. **13**(8): 1054-63.

Lowman, X.H., M.A. McDonnell, A. Kosloske, O.A. Odumade, C. Jenness, C.B. Karim, R. Jemmerson, and A. Kelekar, *The proapoptotic function of Noxa in human leukemia cells is regulated by the kinase Cdk5 and by glucose.* Mol Cell, 2010. **40**(5): 823-33.

Nichols, L.A., L.A. Adang, and D.H. Kedes, *Rapamycin blocks production of KSHV/HHV8: insights into the anti-tumor activity of an immunosuppressant drug.* PLoS One, 2011. **6**(1): e14535.

Pawluczkowycz, A.W., F.J. Beurskens, P.V. Beum, M.A. Lindorfer, J.G. van de Winkel, P.W. Parren, and R.P. Taylor, *Binding of submaximal C1q promotes complement-dependent cytotoxicity (CDC) of B cells opsonized with anti-CD20 mAbs ofatumumab (OFA) or rituximab (RTX): considerably higher levels of CDC are induced by OFA than by RTX.* J Immunol, 2009. **183**(1): 749-58.

Peslak, S.A., J. Wenger, J.C. Bemis, P.D. Kingsley, J.M. Frame, A.D. Koniski, Y. Chen, J.P. Williams*, et al.*, *Sublethal radiation injury uncovers a functional transition during erythroid maturation.* Exp Hematol, 2011. **39**(4): 434-45.

Petrovas, C., B. Chaon, D.R. Ambrozak, D.A. Price, J.J. Melenhorst, B.J. Hill, C. Geldmacher, J.P. Casazza*, et al.*, *Differential association of programmed death-1 and CD57 with ex vivo survival of CD8+ T cells in HIV infection.* J Immunol, 2009. **183**(2): 1120-32.

Praveen, K.S., S. Rajesh, R.N. Kristian, W.E. John, E.G. William, and S. Shailesh, *CCR9 mediates PI3K/AKT-dependent antiapoptotic signals in prostate cancer cells and inhibition of CCR9-CCL25 interaction enhances the cytotoxic effects of etoposide.* International Journal of Cancer, 2010. **9999**(9999): NA.

Reboulet, R.A., C.M. Hennies, Z. Garcia, S. Nierkens, and E.M. Janssen, *Prolonged antigen storage endows merocytic dendritic cells with enhanced capacity to prime anti-tumor responses in tumor-bearing mice.* J Immunol, 2010. **185**(6): 3337-47.

Rees, P., M.R. Brown, H.D. Summers, M.D. Holton, R.J. Errington, S.C. Chappell, and P.J. Smith, *A transfer function approach to measuring cell inheritance.* BMC Syst Biol, 2011. **5**: 31.

Riddell, J.R., X.Y. Wang, H. Minderman, and S.O. Gollnick, *Peroxiredoxin 1 stimulates secretion of proinflammatory cytokines by binding to TLR4.* J Immunol, 2010. **184**(2): 1022-30.

Singh, S., R. Singh, U.P. Singh, S.N. Rai, K.R. Novakovic, L.W. Chung, P.J. Didier, W.E. Grizzle*, et al.*, *Clinical and biological significance of CXCR5 expressed by prostate cancer specimens and cell lines.* Int J Cancer, 2009. **125**(10): 2288-95.

Smith, J., R.P. Bunaciu, G. Reiterer, D. Coder, T. George, M. Asaly, and A. Yen, *Retinoic acid induces nuclear accumulation of Raf1 during differentiation of HL-60 cells.* Exp Cell Res, 2009.

Summers, H.D., P. Rees, M.D. Holton, M. Rowan Brown, S.C. Chappell, P.J. Smith, and R.J. Errington, *Statistical analysis of nanoparticle dosing in a dynamic cellular system.* Nat Nanotechnol, 2011. **6**(3): 170-4.

Yan, Y., A.P. Johnston, S.J. Dodds, M.M. Kamphuis, C. Ferguson, R.G. Parton, E.C. Nice, J.K. Heath*, et al.*, *Uptake and intracellular fate of disulfide-bonded polymer hydrogel capsules for Doxorubicin delivery to colorectal cancer cells.* ACS Nano, 2010. **4**(5): 2928-36.